Hydrothermally shrunk alumina nanopores and their application to DNA sensing

Pavel Takmakov, Ivan Vlassiouk and Sergei Smirnov*

Received 7th June 2006, Accepted 15th August 2006
First published as an Advance Article on the web 5th September 2006
DOI: 10.1039/b608084g

Hydrothermal treatment of anodized alumina membranes has been known for years and is believed to seal the pores by transforming aluminium oxide into lower density hydroxides. We demonstrate that, at least for 60 nm diameter pores grown from anodization in oxalic acid at 40 V, the hydrothermal treatment significantly shrinks but does not fully seal the nanopores. The pores shrink to a neck of less than 10 nm in diameter and 2–4 μm in length, in which the diffusion coefficient of ions is five orders of magnitude smaller than in the bulk. Because of a high electrolyte resistance through hydrothermally treated shrunken nanopores, they can be used for electrical sensing applications, as demonstrated using the example of DNA sensing. Hybridization of target DNA with a complementary ssDNA covalently immobilized inside the nanopores causes an increase in impedance by more than 50% while a noncomplementary ssDNA has no measurable effect.

1. Introduction

The phenomenon of ionic conductance through nanoporous channels has gained great attention in recent years as a practical tool for hopefully fast, inexpensive and convenient detection of chemical and biological species. This method of detection has several advantages over the existing techniques such as microarrays: it does not require labeling of the analyte molecules and employs a convenient electrical detection.

Several realizations of this technique were offered including the use of single nanopores[1] and nanoporous arrays.[2] Conductance variation of both unmodified pores and changes due to analyte binding have been explored. The latter approach should allow parallel detection of a number of analytes on a single microarray chip, where recognition would rely on specificity of their binding to differently modified spots of the array, similar to standard fluorescent microarrays.

The ionic conductance in nanopores can alter as a result of analyte binding either due to the volume exclusion effect or due to the change in surface charge. In the former case, current through the nanopores reduces when analyte binds to the nanopore walls and thus decreases the effective cross section of the channel. The charge effect is observed when the low ion concentration in the channel makes the Debye length (λ_D) comparable to channel diameter. Binding of charged analytes to the channel walls in this case affects the ion concentration in the pore and thus the resulting conductance. Both schemes require very small nanopores. This is more so for the first case, where it is critical that the pore diameter is comparable to the size of an analyte (for biological molecules it is several nm) in order to have a substantial pore blockage. For the second case, the ratio of λ_D to the pore radius is also important and for measurements under physiological ionic strength ($\sim$0.1 M, $\lambda_D \sim 1$ nm) often required for effective binding, it demands pore diameters in the order of a few nanometers as well.

Realization of this technique in a single channel geometry involves fabrication of devices using not easily accessible processes that might hinder it from wide use.

Alternatively, relatively inexpensive arrays of nanopores, anodized alumina membranes, can be employed. Not only are they cheap to fabricate in large quantities but their surface can be conveniently modified using standard microarray spotting techniques.[3] Because the lengths of such pores do not exceed 100 μm, and there are a huge number of them in parallel, it is more challenging to make the membrane resistance dominate the overall cell impedance.[2] Previously we resolved it by placing the electrodes close to the membrane but this prohibits realization of parallel detection with different electrically addressable spots simultaneously sensing different analytes. Another inconvenience of that scheme, elimination of which would make the technique more attractive, was the use of noble metal electrode(s) on which the oxidation/reduction of electroactive species was monitored.

We explore various schemes for eliminating these disadvantages and making the pore resistance dominant. In particular, we try to adopt the technique of hydrothermal sealing for anodized alumina that has been used for passivation of aluminium and its alloys in industry for over forty years.[4]

In this paper we investigate the ionic conductance through shrunk alumina nanopores and its application to DNA sensing. In the first part, we scrutinize the effect of hydrothermal treatment on nanoporous alumina membranes, usually believed to cause sealing of the pores. We conclude that the treatment produces shrunk pores but does not seal them totally. In the second part, the hydrothermally treated membranes with shrunken pores are utilized for electrical detection of DNA oligomers. The detection scheme is attractive due to the simplicity of sensor preparation, low cost, and straightforward detection requiring neither noble metal electrodes nor a redox pair.

Department of Chemistry and Biochemistry, New Mexico State University, Las Cruces, New Mexico, 88003, USA. E-mail: snsm@nmsu.edu; Fax: +1-505-646-2649; Tel: +1-505-646-1547

2. Experimental

Highly ordered nanoporous aluminium oxide membranes were produced *via* two-step anodization as described elsewhere.[5] Briefly, aluminium foil (0.1 mm thick, Puratronic 99.997% aluminium) was first electropolished in an ethanol solution of $HClO_4$ and then anodized in 3% oxalic acid solution at a constant potential of 40 V for 3 h at 7 °C. The oxide layer was removed by CrO_3–H_3PO_4 (1.8% CrO_3 + 6% H_3PO_4) solution and the final anodization was performed under the same conditions to reach a desired pore length. Such a procedure yields 60 nm diameter hexagonally ordered nanopores of 10 μm length (in 3 h of anodization). Hydrothermal treatment was carried out in boiling distilled water for different periods of time eventually causing pores to shrink.[6] No further changes were observed for boiling over 40 min.

Electron micrographs of uncoated as well as gold sputtered samples were taken using Hitachi S-5200 Nano SEM.

Immobilization of single stranded DNA (ssDNA) molecules on the pores' surface followed previously described procedure using aminosilane–glutaraldehyde chemistry[3], sketched in Scheme 1. Briefly, the membranes were washed and dried in air and then 'aminated' for 1 h in 5% toluene solution of aminopropyltrimethoxysilane (both from Aldrich). After rinsing in toluene and baking at 120 °C for 20 min, the procedure was repeated and concluded with overnight baking. Aminated membranes were activated in an 8% aqueous solution of glutaraldehyde for 12 h, rinsed with water and dried. DNA immobilization on the activated surface immediately followed: 5′-aminated 21-mer ssDNA (Integrated DNA Technologies) of the sequence 5′-GCTTAGGATCATCGAG GTCCA-3′ was immobilized from the DI water and washed.

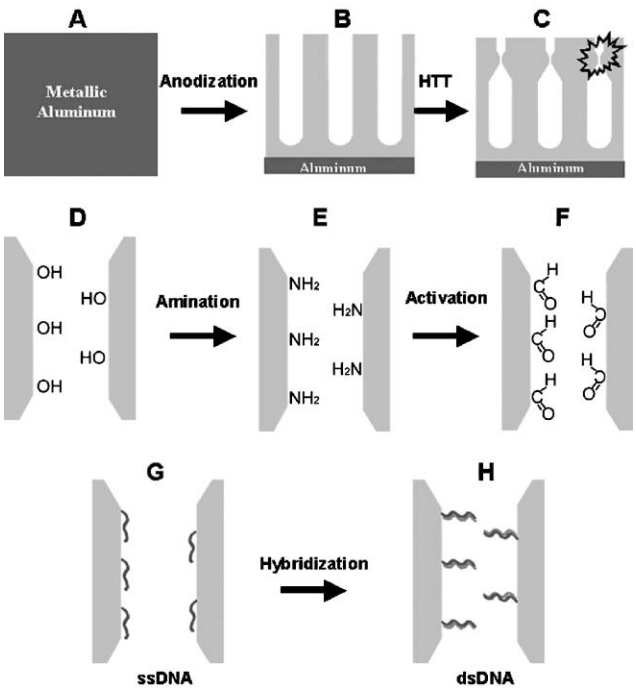

Scheme 1 Aluminium foil was anodized (A to B) and then hydrothermally treated (B to C) in boiling water. Modification of the pores' walls is shown for the black marked area at C. Aminopropyltrimethoxysilane reacted with OH surface groups (D to E) and resulting amino groups were reacted with glutaraldehyde (E to F). Amino terminated 21-mer ssDNA was immobilized by reacting with surface aldehydes (F to G) and hybridization with complementary analyte DNA can be performed.

Complementary 21-mer ssDNA and non-complementary 41-mer ssDNA (5′-ATCTGACTCCTGAGGAGAAGTCT-GCCGTTACTGCCCTGT-3′) were used for the hybridization experiment. Dehybridization was done by soaking the sample in 9 M urea solution.

Electrical impedance was measured at 1 mV AC amplitude in the frequency range from 1 to 10^5 Hz using a CH Instrument 604B potentiostat in a home-made cell using a two-electrode scheme with the back layer of aluminium under the membrane as a working electrode and a polished aluminium rod as the counter electrode immersed in electrolyte solution approximately 3 mm above the membrane. Solutions of KCl at various concentrations (from 10 mM to 3 M) at either pH = 7.0 or in 0.1 M acetate buffer (pH = 5.0) were used as electrolyte. The active membrane area was 0.79 cm^2.

In the dye diffusion experiment, 10^{-4} M solution of Oregon Green 488 (Molecular Probes) in 0.1 M Tris buffer (pH = 7.6) was used as a seed solution to diffuse into the nanoporous membrane. Two halves of the same membrane, one of which was hydrothermally treated and the other not, were glued with epoxy to a glass slide and soaked in the dye solution for different lengths of time and then analyzed under the fluorescent microscope. Since dye diffuses equally slowly into and out of the shrunk membrane, one can monitor the time of dye intake into the membrane if the solution above the membrane is rinsed off quickly before measurements. Prior to each measurement, the sample was rinsed with copious amounts of Tris buffer in order to remove the excess dye and the measurements were done within 1 min after that. Membranes were analyzed using a Carl-Zeiss Axiovert 200 M inverted fluorescent microscope and an AxioCam MRm monochromic digital camera equipped with a filter assembly for Oregon Green 488 dye: HQ 470/40 – excitation, and HQ 525/50 – luminescence to match the dye's absorption and emission maxima at 490 nm and 514 nm, respectively. The exposure time was set at 30 ms for all samples.

3. Results and discussion

3.1. Effect of hydrothermal treatment on pore geometry

Boiling of anodized alumina membranes leads to a partial blockage of their pores. This process has been used for a long time as a way to preserve aluminium from corrosion and make it colored. It is believed to be related to phase transition from γ-Al_2O_3 (specific density 3.65 g cm^{-3}) to boehmite (specific density 3.03 g cm^{-3}) or even lower density aluminium hydroxides.[6]

Impedimetric measurements are the most sensitive to changes in the pores and have been used for characterization of hydrothermally 'sealed' membranes since the sixties. Fig. 1 and 2 demonstrate the changes in the Bode plots upon hydrothermal treatment (HTT). Untreated anodized membrane shows only two elements in the equivalent scheme necessary to describe the behavior: capacitance of the aluminium oxide barrier layer, C_{bl}, and the solution resistance, R_s. The charge transfer across the barrier layer is immeasurably small and the

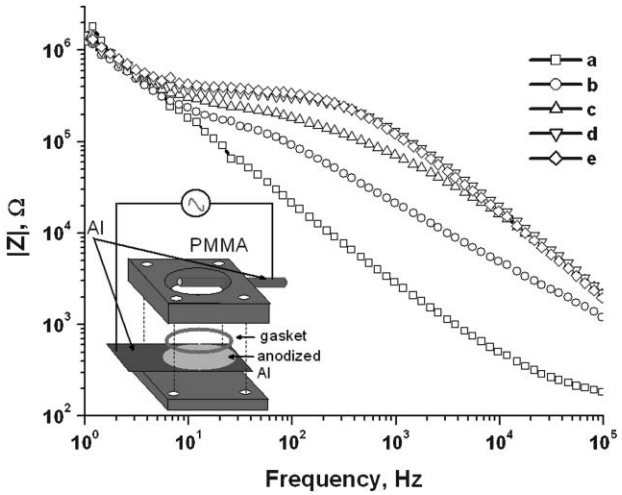

Fig. 1 Impedance Bode plots for nanoporous alumina membranes before and after hydrothermal treatment for different periods of time recorded in 0.1 M KCl: **a** – untreated sample; **b** – treated for 10 min; **c** – treated for 20 min; **d** – treated for 30 min and **e** – treated for 60 min. The inset schematically illustrates the cell.

solution resistance contribution from outside the membrane, R_s, drops linearly with KCl concentration (Fig. 2). HTT membranes, on the other hand, demonstrate more complicated behavior. A short hydrothermal treatment causes gradual increase of the pore resistance and the capacitance. They both eventually arrive at stationary values (see Fig. 1) independent of further prolonging the treatment. The equivalent scheme for the saturated case can be represented with only two additional parameters: resistance of the pores, R_p, and their capacitance, C_p. The solution resistance is not visible any more for HTT membranes because the capacitive contribution to impedance from C_p is greater even at the highest frequencies in our frequency range. The value of the plateau from R_p shows no dependence on the electrolyte concentration and is usually considered as an indication of pores' sealing. Indeed, the

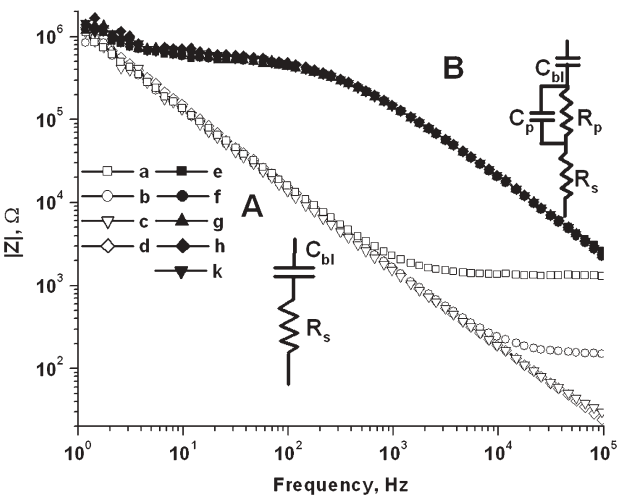

Fig. 2 Impedance Bode plot of untreated (A) and hydrothermally shrunk (B) nanoporous alumina membrane recorded at different concentrations of KCl: 0.01 M (**a** and **e**); 0.1 M (**b** and **f**); 1 M (**c** and **g**); 3 M (**d** and **h**) and 0.1 M acetate buffer (**k**). Inserts show equivalent schemes used for fitting of the two cases.

plateau stays unchanged beyond 40 min of hydrothermal treatment. At the same time, there is no unambiguous explanation for the value of this resistance, *ca.* 0.5 MΩ cm^2. The corresponding capacitance of this 'sealed' portion is in the order of 1 nF cm^{-2} and appears to be independent of the overall pore length or the duration of HTT. Such capacitance corresponds to a dielectric layer with a thickness in the order of a few micrometers (depending on its dielectric constant), which is smaller than the total depth of the pores.

The mechanism of pore sealing is not totally transparent and requires further investigation. It could be important for delineating details that the effect is observed only when nanoporous structures remain on the aluminium back layer (or half sealed) and the treatment is given in a continuous mode. Indeed, alternating the 5 min boiling steps with cooling to room temperature to accrue an overall boiling time of much longer than 40 min never shows the same effect as a continuous 40 min treatment. Similarly, free standing membranes with the aluminium back layer removed and subjected to hydrothermal treatment do not show any sign of sealing even if boiled continuously for over 2 h. Thus it appears that the 'sealing' takes place as a result of concentration build up inside the pores, which is probably accompanied by a pressure increase and maybe a local change of pH.

What we will try to prove below is that such HTT membranes are not fully sealed. Along the way, we will describe what R_p corresponds to and why it does not depend on the electrolyte concentration. We start with a qualitative justification of the pores' existence using diffusion of a fluorescence dye (Oregon Green). Diffusion of the dye into untreated membranes is not hindered and happens within seconds. The diffusion time, τ, according to eqn (1):

$$\tau \sim \frac{L^2}{D} \tag{1}$$

for L = 10 μm long pores and the diffusion coefficient, $D \sim 10^{-9}$ m^2 s^{-1}, is only ~ 0.1 s. Thus, it takes an equally short time for dye to diffuse in and out of the pores. If diffusion into HTT membranes happens but with a smaller diffusion coefficient, then HTT membranes exposed for a long enough time to the dye solution should retain it after a quick rinsing with a buffer, while untreated membranes should be completely cleared of the dye upon rinsing.

The results of this experiment are shown in Fig 3. Untreated membranes appear dark, as expected for fast dye diffusion out. Brightness of HTT membranes, on the other hand, is significantly greater, *i.e.* HTT membranes are not fully sealed but are rather shrunk with much smaller diameters and substantially slow diffusion of the dye. The timescale for this diffusion can be determined from the kinetics of the fluorescence intensity growth. According to Fig. 3, the brightness saturates at *ca.* 10 min, giving the characteristic diffusion time into pores.

SEM examination of HTT membranes given in Fig. 4 shows that most of the pores' mouths are not sealed completely on the surface of the membrane (Fig. 4A) but the side view (Fig. 4B) indicates that below ~0.5 μm in depth from the surface of HTT membrane, the porous structure almost disappears (region D in Fig. 4B). Region C in Fig. 4A

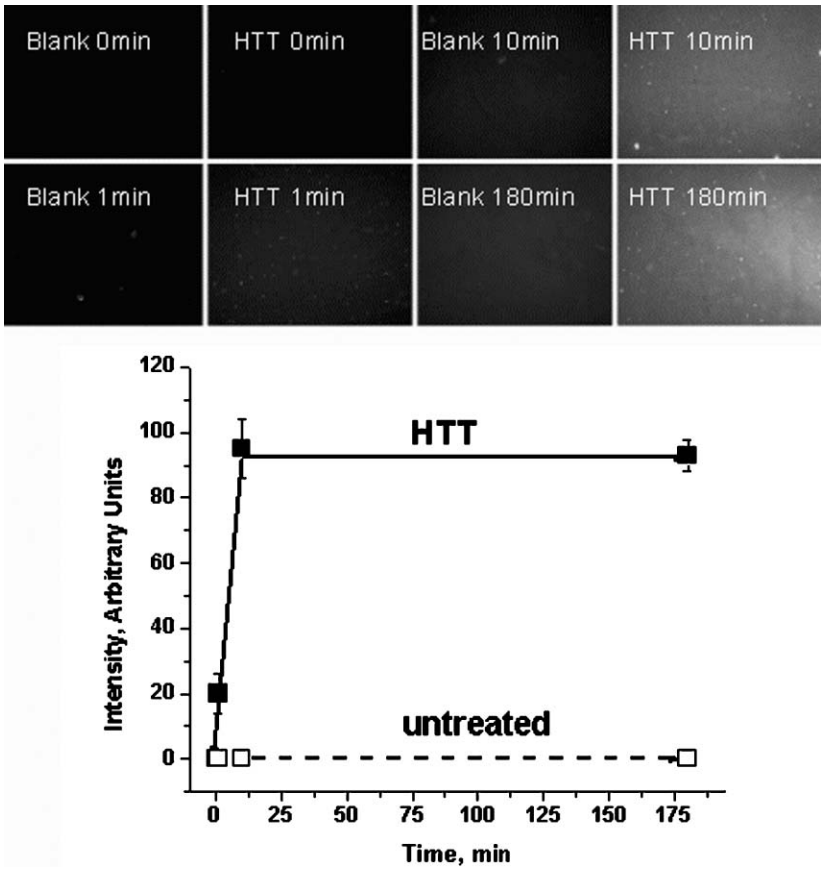

Fig. 3 Fluorescence microscope images of the Oregon Green transport into blank and HTT nanoporous membranes after different exposure times (0, 1, 10 and 180 min).

demonstrates a horizontal break at approximately that depth, where pore blockage is visibly protruding.

Now that we have established that pores are not sealed but shrunk, it is time to rationalize the observed parameters quantitatively. The values of variables obtained from the fittings using the equivalent scheme shown in Fig. 2 are given in Table 1. Most intriguing is the lack of R_p dependence on the electrolyte concentration up to 3 M KCl. It has been shown before[1] that conductance in the small diameter pores ceases its declining with lowering electrolyte concentration and eventually saturates. This happens when the surface charge on the pore walls enforces the concentration of counter ions in the pore to exceed the bulk concentration of ions, C_{bulk}:

$$c_{bulk} < \frac{2\sigma_{charge}}{r} \quad (2)$$

where σ_{charge} is the surface charge density on the pore walls, and r is the pore radius. The pore radii in the experiments of Stein *et al.*[1] exceeded 70 nm and the electrolyte concentrations, for which inequality of eqn (2) became opposite, was relatively small, in the order of 10 mM. Is it possible to sustain the conditions of eqn (2) at $C_{bulk} \sim 3$ M? We speculate that it is possible. The surface charge density can be estimated based on the solution pH, the surface density of OH groups, σ_{OH}, on the aluminium oxide, and its pH of zero charge (pH_{zc}). The surface density of OH groups can be conservatively estimated as $\sigma_{OH} = 5\ nm^{-2}$,[7] but the density can be even higher for lower density

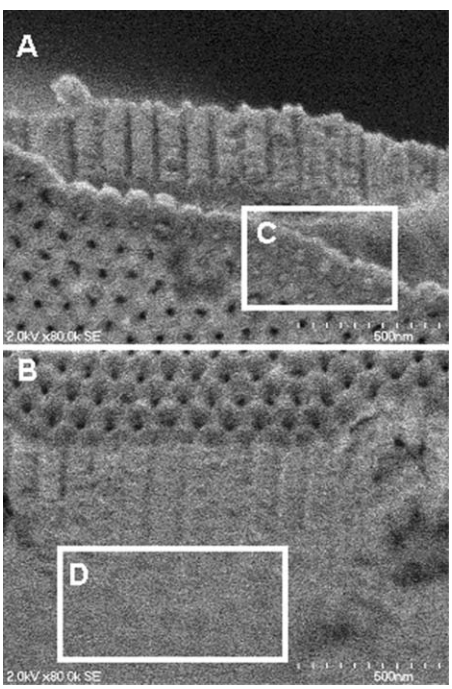

Fig. 4 SEM micrographs of HTT nanoporous alumina membrane. Top view (A) and the side view (B) show the shrunk pore zone (labeled as C and D regions) developed inside the porous structure.

Table 1 Fitting parameters for the curves in Fig. 5 using the equivalent scheme from the insert of Fig. 2:

	R_s[a]/Ω cm^{-2}	C_{bl}[b]/μF cm^{-2}	R_p[c]/kΩ cm^{-2}	C_p[d]/pF cm^{-2}
Blank membrane	291 ± 11	0.120 ± 0.024	N/A	N/A
Shrunk membrane	N/A	0.109 ± 0.078	502 ± 18	888 ± 30
With immobilized ssDNA	N/A	0.085 ± 0.007	220 ± 11	922 ± 45
With complementary DNA (dsDNA)	N/A	0.112 ± 0.043	352 ± 8	859 ± 19
After denaturing dsDNA with urea	N/A	0.122 ± 0.005	241 ± 6	919 ± 22
With non-complementary DNA	N/A	0.129 ± 0.005	243 ± 6	998 ± 27

[a] Solution resistance. [b] Barrier layer capacitance. [c] Pore resistance. [d] Pore capacitance.

aluminium hydroxides. Based on the literature value of pH_{zc} = 8.5–9,[8] one can conclude that for pH < 7.5 more than 90% of surface hydroxyls are protonated, *i.e.* positively charged. For $\sigma_{charge} \sim 3$ nm^{-2}, the high limit estimate for the pores' radius that would satisfy conductance independence of electrolyte concentrations at 3 M, is $r < 3$ nm. Note that this is just a high limit estimate and can be quite different from the actual pores' diameter. It can, and likely is, noticeably smaller, which explains why SEM does not have sufficient resolution to identify the shrunken pores.

The length of the zone with shrunk pores, l, can be estimated from the pore capacitance, C_p, (see Table 1) *via* the expression:

$$l = \frac{\varepsilon\varepsilon_0 \alpha A_{cell}}{C_p} \quad (3)$$

where ε is the dielectric constant of the shrunken zone, ε_0 is the dielectric permittivity of the vacuum; α is the pore surface coverage ($\sim$0.65 for the anodization conditions used) and A_{cell} is the membrane area. Using ε = 9.0, of aluminium oxide, as the high limit, puts the upper limit estimate of $l < 4$ μm. Lower density aluminium hydroxides can have an ε as low as 4.5,[9] making the lower limit estimate $l > 2$ μm.

Based on the above estimates of pores' geometry (r and l) the specific resistance, ρ, of the shrunken portion can be estimated from the resistance R_p and the surface density of pores, $N_p \sim 10^{14}$ pores m^{-2}:

$$\rho = \frac{R_p N_p A_{cell} \pi r^2}{l} \quad (4)$$

For $r < 3$ nm and $l > 2$ μm it corresponds to $\rho < 10^4$ Ω m. For comparison, the specific resistance of bulk 3 M KCl is about $\sim$0.03 Ω m, almost six orders of magnitude less than the above estimate. The difference suggests a much lower diffusion coefficient for electrolyte ions inside the pores, D_p. Since the specific resistance is inversely proportional to the diffusion coefficient (Fick's Law) one can estimate a lower limit for the diffusion coefficient of electrolyte ions (estimated for the high limit of r = 3 nm) as low as $D_p > 4 \times 10^{-15}$ m^2 s^{-1}. Alternatively, one can independently estimate D_p using the diffusion time ($\tau_p \sim 10$ min) for the dye through the shrunk pores: $D_p \sim L^2/\tau_p$ (see eqn (1)). Using data from the fluorescence kinetics and neglecting (for the sake of simplicity) the difference between the dye and the ions of the electrolyte, the diffusion coefficient limits can be estimated as $D_p \sim 7$–30×10^{-15} m^2 s^{-1}, in a relatively good agreement with the estimates from R_p. The best overlap for all parameters happens for $r \sim 1.5$–2 nm, $l \sim 2$ μm, and $D_p \sim 10^{-14}$ m^2 s^{-1}. Alternatively, if the shrinkage proceeds *via* blocking the pores with nanoparticles, the area of resulting gaps can be larger than πr^2, which would result in slightly smaller values of r and D_p.

It should not be surprising to see a so dramatically decelerated diffusion constant in small nanopores. The interface between the electrolyte and the charged surface has significantly altered properties from those in the bulk; even water density is apparently increased.[10] The viscosity of liquids, including water, was reported to be higher than that in the bulk by many orders of magnitude in nanometer size confinements.[11]

3.2. DNA detection

Since the shrunken pores appear of a quite small size, one can construct a sensor element built on the conductance variation through these membranes. We chose DNA as the already established platform[2] but demonstrate here that, because of a much smaller pore size, electrical detection can be realized without any electrochemical pair and without noble electrodes.

First, immobilization of ssDNA inside the nanopores leads to a significant decrease in R_p (see Table 1) as compared to unmodified HTT membrane. This may be explained as a consequence of the increased surface charge density (of opposite sign) from the negatively charged DNA backbone and possible partial dissolution during the multistep procedure of DNA immobilization. A similar variation in the membrane resistance after modification was observed in 20 nm membranes and monitored by conductance of ferricynaide and Ru hexamine.[2] There are as many as 21 charges for each OH group from the immobilized ssDNA 21-mer. Even though almost all OH groups are likely neutralized/modified as a result of silanization/activation steps, not all of them are eventually replaced with ssDNA: maximum surface density of ssDNA, obtained using this immobilization procedure is about 0.04 nm^{-2}.[2,3]

Hybridization of immobilized ssDNA with a complementary strand leads to an increased R_p with double stranded DNA (dsDNA), which nevertheless is lower than without any DNA. The effect is similar to that previously reported[2] but now the detection is realized without a redox pair (just with electrolyte) and using aluminium electrodes. As before, we speculate that the R_p changes due to the volume exclusion blockage in the pores, which hinders the ionic current.[2] The effect is probably accompanied by a change in DNA orientation with respect to the surface—more stiff dsDNA should likely lift up away from the surface and hinder the diffusion to a greater extent.[12] The effect is counteracted by increased surface charge but, apparently, the latter has a comparatively smaller contribution than the change in electrolyte diffusion. It required more than two hours for completion of the hybridization step, as monitored by the

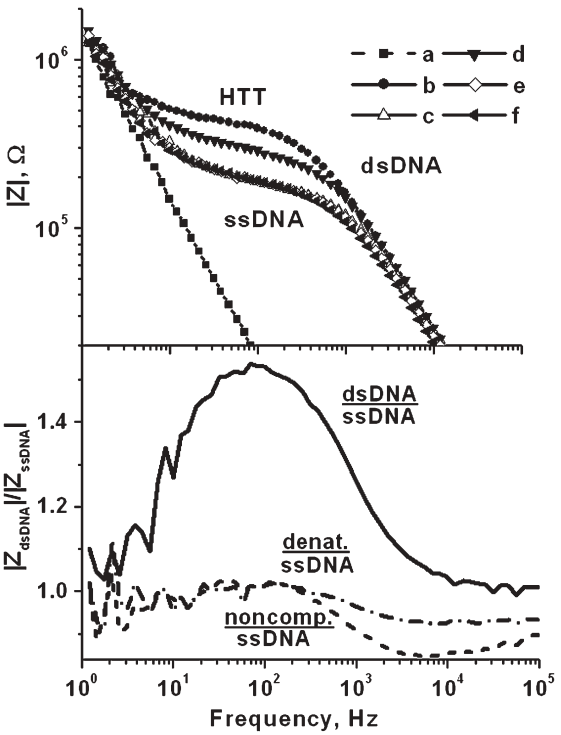

Fig. 5 **Top**: impedance Bode plot for nanoporous alumina membrane recorded in 0.1 M KCl solution: **a** – untreated membrane; **b** – membrane after hydrothermal treatment (HTT); **c** – HTT membrane after immobilization of ssDNA; **d** – after hybridization with complementary ssDNA; **e** –after dehybridization with urea; **f** –with noncomplementary ssDNA. **Bottom**: relative change of impedance after hybridizing with complementary (solid) and noncomplementary (dashed) analyte DNA; dot-dashed line shows the ratio for impedances before hybridization and after denaturing dsDNA with urea. The noise at low frequencies diminishes when higher AC amplitudes are used.

conductance decline. This is not surprising given the slow diffusion of ions into the shrunken pores and even slower anticipated diffusion of 21mer ssDNA oligomer.

Denaturing of dsDNA by urea releases the bound complementary DNA strands and leads to a full recovery of R_p to the initial value observed for immobilized ssDNA (Fig. 5 and Table 1). At the same time, a non-complementary ssDNA has no significant effect on the resistance (Fig. 5 and Table 1). Combination of these observations leads us to believe that the effect is selective and takes place only as a result of sequence-specific hybridization between the immobilized ssDNA and the complementary target ssDNA, *i.e.* the conductance variation can be used for detecting DNA (and RNA) targets.

Extended treatment of the same membrane (hybridization, denaturing with urea, and 12 h exposure to noncomplementary DNA solution in Fig. 5) probably disturbs the integrity of pores. The signs of 'wearing' are visible in Fig. 5 (see also Table 1) as incomplete recovery of impedance to the original value: the ratio of impedances after denaturing and before hybridization becomes less than unity and further decreases after extended treatment in solution with noncomplementary DNA. The effect emerges mostly as increasing pore capacitance but requires further investigation.

Since the pore resistance dramatically exceeds that of the electrolyte, this technique opens an attractive opportunity of realizing it in a microarray format: patterned arrays of aluminium electrodes can be individually anodized and uniquely modified with different DNA or other biomolecules. These electrodes can be independently addressed against a common counter electrode. Independence of electrolyte concentration offers additional advantages in such an application.

4. Conclusions

We have shown that anodized alumina membranes exposed to hydrothermal treatment undergo significant shrinking but not full sealing of nanopores. The original 60 nm diameter pores shrink to a neck of approximately 5–10 nm in diameter and 2–4 μm long, where the diffusion coefficient of ions is five orders of magnitude smaller than that in the bulk. Because of a high resistance through such small size pores, hydrothermally treated membranes can be used for electrical sensor applications. Hybridization of target DNA with covalently immobilized ssDNA inside the pores causes an increase in impedance by more than 50%.

Acknowledgements

This work was supported by a grant from the National Institutes of Health (NIH SCORE GM08136). We thank Dr Dmitri Brevnov for help with SEM imaging.

References

1 D. Stein, M. Kruithof and C. Dekker, *Phys. Rev. Lett.*, 2004, **93**, 035901; R. Karnik, K. Castelino, R. Fan, P. Yang and A. Majumdar, *Nano Lett.*, 2005, **5**, 1638; Z. Siwy, L. Troffin, P. Kohli, L. A. Baker, C. Trautmann and C. R. Martin, *J. Am. Chem. Soc.*, 2005, **127**, 5000.
2 I. Vlassiouk, P. Takmakov and S. Smirnov, *Langmuir*, 2005, **21**, 4776.
3 I. Vassiouk, A. Krasnoslobodtsev, S. Smirnov and M. Germann, *Langmuir*, 2004, **20**, 9913; V. Szczepanski, I. Vlassiouk and S. Smirnov, *J. Membr. Sci.*, 2006, **281**, 587; P. Takmakov, I. Vlassiouk and S. Smirnov, *Anal. Bioanal. Chem.*, 2006, **385**, 954.
4 E. F. Barkman, *Anodized aluminum: a symposium presented during Committee Week*, Cleveland, Ohio, February 9, American Society for Testing and Materials, Philadelphia, PA, 1965.
5 A. P. Li, F. Muller, A. Birner, K. Nielsch and U. Gosele, *J. Appl. Phys.*, 1998, **84**, 6023; H. Masuda and K. Fukuda, *Science*, 1995, **268**, 1466.
6 T. P. Hoar and G. C. Wood, *Electrochim. Acta*, 1962, **7**, 333; V. Lopez, M. J. Bartolome, E. Escudero, E. Otero and J. A. Gonzalez, *J. Electrochem. Soc.*, 2006, **153**, B75.
7 P. Tundo, P. Venturello and E. Angeletti, *J. Am. Chem. Soc.*, 1982, **104**, 6551; H. Brunner, T. Vallant, U. Mayer, H. Hoffman, B. Basnar, M. Vallant and G. Friedbacher, *Langmuir*, 1999, **15**, 1899; S. R. Wasserman, Y. T. Tao and G. M. Whitesides, *Langmuir*, 1989, **5**, 1074; A. Tuel, H. Hommel, A. P. Legrand and E. Kovats, *Langmuir*, 1990, **6**, 770; F. Vigne-Maeder and P. Sautet, *J. Phys. Chem. B*, 1997, **101**, 8197; A. Krasnoslobodtsev and S. Smirnov, *Langmuir*, 2001, **17**, 7593.
8 E. A. El-Katatny, S. A. Halawy, M. A. Mohamed and M. I. Zaki, *Powder Technol.*, 2003, **132**, 137.
9 Y. C. Wang, I. C. Leu and M. H. Hon, *J. Appl. Phys.*, 2004, **95**, 1444.
10 G. Cicero, J. C. Grossman, A. Catellani and G. Galli, *J. Am. Chem. Soc.*, 2005, **127**, 6830.
11 Y. Zhu and S. Granick, *Phys. Rev. Lett.*, 2001, **87**, 096104; K. B. Jinesh and J. W. M. Frenken, *Phys. Rev. Lett.*, 2006, **96**, 166103.
12 T. Hianik, V. Gajdos, R. Krivanek, T. Oretskaya, V. Metelev, E. Volkov and P. Vadgama, *Bioelectrochemistry*, 2001, **53**, 199; X. Yang, Q. Wang, K. Wang, W. Tan, J. Yao and H. Li, *Langmuir*, 2006, **22**, 5654.